The rotation number in one-dimensional maps: definition and applications

2006 J. Phys. A: Math. Gen. 39 15231

(http://iopscience.iop.org/0305-4470/39/49/011)

INSTITUTE OF PHYSICS PUBLISHING JOURNAL OF PHYSICS A: MATHEMATICAL AND GENERAL

J. Phys. A: Math. Gen. **39** (2006) 15231–15244 doi:10.1088/0305-4470/39/49/011

The rotation number in one-dimensional maps: definition and applications

G Livadiotis[1] **and N Voglis**[1,2]

[1] Section of Astronomy, Astrophysics and Mechanics, Department of Physics, University of Athens, Panepistimiopolis, GR-15784 Zografos, Athens, Greece
[2] Research Center for Astronomy and Applied Mathematics, Academy of Athens, Soranou Efessiou 4, GR-15669 Athens, Greece

E-mail: glivad@phys.uoa.gr and nvogl@academyofathens.gr

Received 27 July 2006, in final form 18 October 2006
Published 21 November 2006
Online at stacks.iop.org/JPhysA/39/15231

Abstract

A rotation number in the case of one-dimensional maps is introduced. As is shown, this rotation number is equivalent to the already known rotation number in the case of two-dimensional maps. The definition of the rotation number is given in two steps. First, it is defined for periodic orbits inside a window of organized motion (WOM). We show that in this case our definition coincides with the definition of the over-rotation number. Then, our definition is further generalized for chaotic orbits outside the WOMs. Thus, we obtain a unified definition of the rotation number for the whole area of the chaotic zone of the bifurcation diagram, having a number of useful applications. Namely, it can be used as a tool to distinguish whether an orbit is contained within a WOM or not, as a tool of numerical location of the bifurcation points, of the band mergings, as well as of the boundary points of a WOM. Finally, a method of numerical calculation of the percentage of the cumulative width of the WOMs in every particular segment (chaotic band) of the chaotic zone is given.

PACS numbers: 05.45.−a, 02.30.Oz, 05.45.−a, 05.45.Ac

1. Introduction

One-dimensional maps are defined as $x_{n+1} = f(x_n; p)$, where p is the control parameter and $x_n = f^n(x_0; p)$ is the nth iteration of this map with the initial point x_0. A typical example is the logistic map

$$f(x_n; p) = p \cdot x_n \cdot (1 - x_n). \tag{1}$$

It is well known that the bifurcation diagram of this map is separated into two main zones, namely the main zone of order, for which $p < p_\infty$, and the main zone of chaos, where $p > p_\infty$

with p_∞ defined as the boundary point between these two zones, called Feigenbaum's point, (see, for example, Kapitaniak (2000)).

The main zone of order contains no chaotic attractors. It is characterized by point attractors and point repellers. Any initial condition in this zone gives an orbit that tends asymptotically to coincide with a point attractor, performing regular motion. For this reason these attractors are also called asymptotically stable attractors. On the other hand, the main zone of chaos contains chaotic attractors along the control parameter p, which are interchanged by windows of values of p where point attractors and point repellers of various multiplicities appear. These point attractors and point repellers form a secondary zone of order. Every branch of a multiple point attractor ends up with a 'tail' of a secondary zone of chaos. Any initial condition in these windows tends asymptotically to coincide with either a point attractor or the secondary zone of chaos. Even when orbits tend asymptotically to chaotic attractors of the secondary chaotic zones, they give a general impression of regular motion. For this reason these windows are often called windows of organized motion or WOMs, for short. (Note that within a WOM the secondary zones of order and chaos reproduce in smaller scales, in a 'miniature', the whole topology of the bifurcation diagram. See, for example, Peitgen *et al* (1992), Alligood *et al* (1996)).

Throughout this paper, the terms zones of order and chaos refer to the main ones, i.e. those of the main bifurcation diagram, not the respective secondary zones inside the WOMs. The topology of the zone of order in the bifurcation diagram is characterized by asymptotically stable periodic attractors with period N to be given by multiples of 2, that is $f^N(x;\, p) = x$, $N = 2^k, \forall\, k \in \aleph$, where $\aleph$ is the set of physical numbers. This general property of the zone of order of the bifurcation diagram of any one-dimensional map has been shown by Li and Yorke (1975). The arrangement of these attractors with increasing p is described as the period-doubling cascade, in which two new branches out of an initial branch appear and the period doubles.

The values of p, at which the subsequent bifurcations occur, are called bifurcation points $p_0, p_1, p_2, \ldots, p_k, \ldots, p_\infty$. In the interval (p_k, p_{k+1}) only attractors of period 2^k can be realized, therefore 2^k branches appear as a function of p, one for each iteration. The serial number k is called generation of these branches.

Asymptotically stable periodic attractors appear also within WOMs in the zone of chaos. Their period N is not necessarily given by multiples of 2, that is $f^N(x;\, p) = x$, $N(\geqslant 3) \in \aleph$. They are often called tangent attractors, because their first branch begins by tangent bifurcation. In a tangent bifurcation a pair of stable and unstable periodic orbits (attractor and repeller respectively) of multiplicity N appears abruptly out of chaos (for further detail see Guckenheimer and Holmes (1997)). The multiplicity N is often called the period of the WOM.

In addition, referring to the periodic attractors with Nth multiplicity, we mean the asymptotically stable periodic orbits of a period N.

The onset of a particular WOM of a period N occurs at a critical value of the control parameter $p = w_{N,1}$, where chaos is abruptly replaced by a tangent attractor with multiplicity N. Furthermore, as p increases inside the WOM, every one of the N branches of the Nth multiplicity attractor evolves to a secondary bifurcation diagram, producing as a whole N miniatures of the main diagram, as mentioned above. These N miniatures end up at another critical value of $p = w_{N,2}$, where the corresponding secondary chaotic zones are abruptly replaced by the extended chaos of the main diagram. On the left-hand side of each WOM, $p < w_{N,1}$, and for values of p quite close to $w_{N,1}$, the orbits (although they are chaotic) present segments with quasi-organized motion with the period quite close to the period of the WOM. This effect is known as intermittency. Then again, on the right-hand side of each WOM,

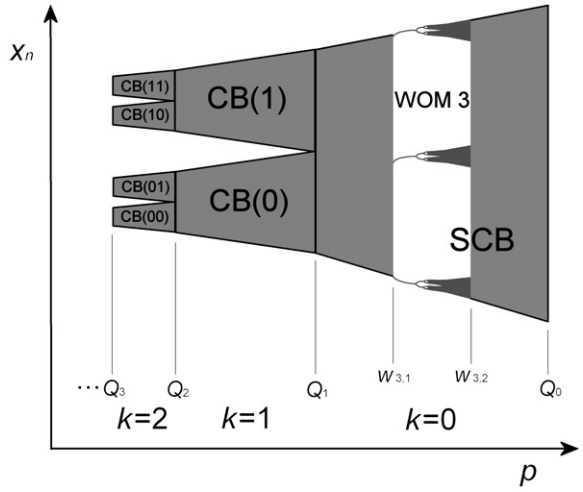

Figure 1. Sketch of a chaotic zone. The doubling of CBs, as p decreases, and their binary labelling system is shown. The WOM of period 3 with its boundary values, $w_{3,1}$ and $w_{3,2}$, is shown for the SCB. The generation, k, and the band mergings, $p = Q_k$, are also indicated (in the case of the logistic map: $Q_0 = 4$, $Q_1 = 3.678\,573\,510\,428\,320\ldots$, $Q_2 = 3.592\,572\,184\,106\,979\ldots$, $Q_3 = 3.574\,804\,938\,759\,209\ldots$, etc).

$p > w_{N,2}$, and for values of p quite close to $w_{N,2}$, the orbits present segments of motion that mimics approximately the motion on the secondary chaotic zones of the WOM. This effect is known as crisis. (See, for example, Kapitaniak (2000), Lichtenberg and Lieberman (1992), Peitgen *et al* (1992), Post *et al* (1989).) The width of the WOM is measured by the difference $\Delta p_w = w_{N,2} - w_{N,1}$. In the schematic representation of figure 1, an illustration of the WOM of period 3 with its boundary values, $w_{3,1}$ and $w_{3,2}$, is demonstrated.

The chaotic zone of the main bifurcation diagram can be described by sections named chaotic bands (CBs). Schematically, the sequence of the CBs in the chaotic zone is shown in figure 1. In this figure, a single chaotic band (SCB) is formed in the interval $Q_1 \leqslant p \leqslant Q_0 = 4$. For $Q_2 \leqslant p \leqslant Q_1$, two new CBs are formed, indicated as CB(0) and CB(1). At $p = Q_1$, the SCB is split into these two CBs. Similarly, at $p = Q_2$, CB(0) is split into CB(00) and CB(01), while CB(1) is split into CB(10) and CB(11). This procedure is repeated in the same manner for every CB that follows. A point as $p = Q_1$ at which splitting or merging of CBs occurs is called band merging. The binary system is used to label these CBs, i.e. CB(0), CB(1), CB(00), CB(01), CB(10), CB(11) and so on (Lichtenberg and Lieberman 1992, Peitgen *et al* 1992). The interval of the chaotic zone between Q_{k+1} and Q_k includes 2^n CBs. The serial number k is called generation of the CBs and the period in the interval (Q_{k+1}, Q_k) is 2^k.

The procedure of chaotic bands splittings or mergings is the same for any unimodal one-dimensional map. Unimodal maps constitute a broad category of one-dimensional maps defined on the interval [0, 1], which have a differentiable maximum and fall off monotonically on both sides. These maps are characterized by a 'structural universality', i.e. the infiniteness of WOMs appears with the same arrangement in all the CBs (Geisel and Nierwetberg 1981, Guckenheimer 1979, Metropolis *et al* 1973, Schuster 1989). In the case of the logistic map, the chaotic zone of the main bifurcation diagram lies in the interval $p_\infty \leqslant p \leqslant 4$ and the mentioned procedure is illustrated in figure 1.

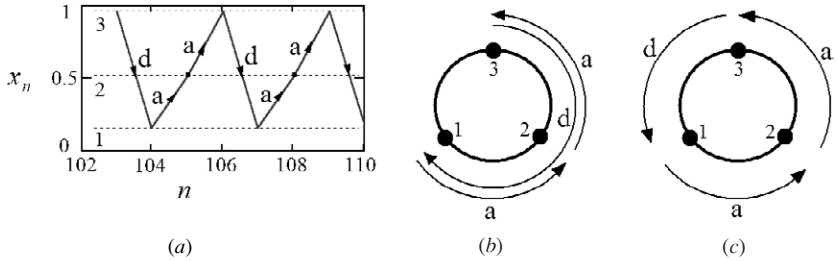

Figure 2. (*a*) The route of the orbit passing through all the three branches of the tangent attractor inside the WOM of period 3 located at $p = w_{3,1} = 3.828\,43\ldots$ for the SCB of the logistic map. (*b*) The respective sketch in the circular representation, where an ascent 'a' is a counterclockwise rotation, while a descent 'd' is a clockwise rotation, and (*c*) the descent is interpreted as a counterclockwise rotation.

In the zone of order we have the doubling of the branches, as p increases, while in the zone of chaos we have a similar doubling of CBs, as p decreases, forming a symbolic mirror symmetry around the Feigenbaum's point, $p_\infty = Q_\infty$.

The whole analysis of this paper can be applied in the case of any unimodal one-dimensional map. Nevertheless, all the numerical results presented in this dissertation correspond to the logistic map.

In section 2 the definition of the rotation number in one-dimensional maps is given, either for orbits inside a WOM or for chaotic orbits outside WOMs. The dependence of the rotation number on the control parameter p is also discussed. We present two alternative methods of investigating whether an orbit is contained in a WOM or not. In section 3 further applications of the rotation number are presented, such as the numerical location of the bifurcation points, of the band mergings, as well as of the boundary points of a WOM. In addition, we present a method of numerical calculation of the percentage of the cumulative width of the WOMs inside a CB. Finally, a summary of conclusions is given in section 4.

2. The rotation number

2.1. Definition of a rotation number for periodic orbits within WOMs

Consider an orbit inside the WOM of period 3. Let the control parameter p belong to the first three branches of generation $k = 0$ of the secondary zone of order, i.e. before the doubling bifurcation of the tangent attractor of multiplicity 3. It is interesting to study in which way the orbit visits all the three branches of the attractor. For the WOM of period 3 this route is simple as is shown below.

Let u be the separation between two successive branches along x (being a constant for simplicity). We consider the highest branch (the branch with the largest value of x) being the initial point of an orbit, labelled by 3 in figure 2(*a*). We choose as starting time the iteration $n = 103$. In the next iteration ($n = 104$), the orbit falls to the lowest branch 1 by a descent of size $2 \cdot u$. Then it continues with an ascent of size $1 \cdot u$ to the attractor 2 ($n = 105$), and with an ascent of size $1 \cdot u$ back to the highest branch 3 ($n = 106$). The step of time, given by iteration, specifies that the reverse procedure, i.e. descents from 3 to 2 to 1 and then an ascent to 3, is not the case.

Furthermore, the three branches can be interpreted as points on a circle separated by equal arcs of angle $u = \Delta\theta_3 = 2\pi/3$. Thereafter, the orbit can be represented as a motion on a

circle, figure 2(*b*), where an ascent is a counterclockwise rotation by an angle of size $\Delta\theta_3$, while a descent is a clockwise rotation by an angle of size $2 \cdot \Delta\theta_3$.

The above descent can also be interpreted as a counterclockwise rotation by the supplementary angle $2\pi - 2 \cdot \Delta\theta_3$. Thus, by this representation the orbit describes constantly a uniform counterclockwise circular motion.

In the WOM of period 3 the orbit describes one complete cycle after three iterations (equal to the number of branches, i.e. the attractor multiplicity), figure 2(*c*). As we show below, the number of the complete cycles described by the orbit in one period of a WOM, is equal to the number of the descents that occur in the same period.

Generally, in a WOM of period N (tangent attractor of multiplicity N), the orbit describes a total number of l descents and a total number of m ascents, so that $N = l + m$.

Since after completing a period, the orbit comes back to the initial branch, it follows that

$$\sum_{i=1}^{l} (-\Delta\theta_{\mathrm{des},i}) + \sum_{j=1}^{m} (\Delta\theta_{\mathrm{asc},j}) = 0, \tag{2}$$

where $\Delta\theta_{\mathrm{des},i}$ denotes the clockwise angle of the orbit's rotation during the ith descent and $\Delta\theta_{\mathrm{asc},j}$ denotes the counterclockwise angle during the jth ascent.

If we replace the clockwise rotation angle $\Delta\theta_{\mathrm{des},i}$ of a descent by an equivalent counterclockwise angle $2\pi - \Delta\theta_{\mathrm{des},i}$, i.e.

$$-\Delta\theta_{\mathrm{des},i} \to 2\pi - \Delta\theta_{\mathrm{des},i}, \tag{3}$$

the total sum of the angles, Θ, becomes

$$\Theta = \sum_{i=1}^{l} (2\pi - \Delta\theta_{\mathrm{des},i}) + \sum_{j=1}^{m} \Delta\theta_{\mathrm{asc},j} = \sum_{i=1}^{l} (2\pi) + \sum_{i=1}^{l} (-\Delta\theta_{\mathrm{des},i}) + \sum_{j=1}^{m} \Delta\theta_{\mathrm{asc},j} = 2\pi \cdot l. \tag{4}$$

Thus, we have shown that, after N periods the orbit describes in its circular representation a total angle $\Theta = 2\pi \cdot l$, equal to l complete cycles, i.e. a number l of cycles equal to the number of descents. Throughout, the number l is denoted by $\mathrm{Des}(N)$.

Therefore, for every WOM of period N, a rational rotation number, ω, can be defined as

$$\omega = \frac{\mathrm{Des}(N)}{N}. \tag{5}$$

Hence, for the case of the WOM of period 3, the rotation number is equal to $\omega = 1/3$.

As another example, consider the WOMs of period 5. In each CB there are three such WOMs, having the following arrangement: two of them lie next to the WOM of period 3, one in each side. The third one appears for greater values of the control parameter, lying on the right-hand side of the WOM of period 4.

Figure 3 shows the circulation of the orbit in every one of the three WOMs of period 5 and their respective description in the circular representation. Both of these WOMs which are next to the WOM of period 3 have a rotation number equal to $\omega = 2/5$, whereas the third WOM of period 5 has a rotation number equal to $\omega = 1/5$.

The idea of using the number of descents as a detection tool has been also applied by Adamopoulos *et al* (1997). Nevertheless, in our analysis we use this idea as a starting point for the definition of the rotation number in one-dimensional maps.

2.2. A generalized definition of the rotation number

It is remarkable that the above definition of the rotation number can be directly derived from the more general definition of the rotation number in two-dimensional maps.

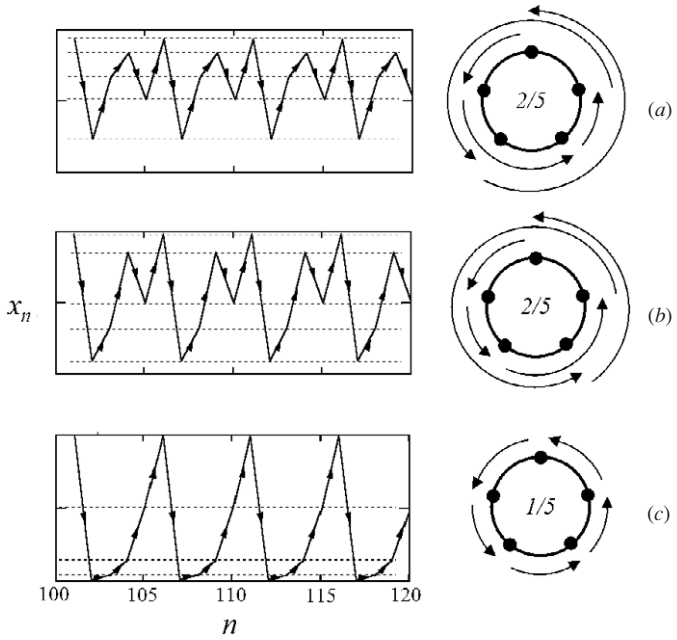

Figure 3. The route of the orbit passing through all the branches of the tangent attractor of multiplicity 5 inside the three WOMs of period 5 for the SCB of the logistic map. Their respective description in the circular representation is also illustrated. The three WOMs of period 5 are arranged as follows: two of them lie next to the WOM of period 3, one in each side, located at $p = w_{5(a),1} = 3.738\,18\ldots$ (a) and $p = w_{5(b),1} = 3.905\,57\ldots$ (b), respectively, with the same rotation number, equal to $\omega = 2/5$. The third one appears for greater values of the control parameter, lying on the right-hand side of the WOM of period 4, located at $p = w_{5(c),1} = 3.990\,26\ldots$, with a rotation number equal to $\omega = 1/5$ (c).

Let $\vec{r}_k$ and $\vec{r}_{k+1}$ be the position vectors of two successive consequents of an orbit (either regular or chaotic) in a two-dimensional map. The origin of the vectors is located at a fixed point of the map. Then, the rotation number, ν_θ, is defined as

$$\nu_\theta = \frac{1}{2\pi} \cdot \lim_{N\to\infty} \frac{1}{N} \sum_{k=1}^{N} \theta_k, \tag{6}$$

where θ_k is the rotation angle, that is the angle between the vectors $\vec{r}_k$ and $\vec{r}_{k+1}$, and N is the number of iterations.

If (6) is applied in the form

$$\nu_\theta = \frac{1}{2\pi} \cdot \frac{1}{N} \sum_{k=1}^{N} \theta_k, \tag{7}$$

where N is the period of a periodic orbit, and the total angle of rotation, $\sum_{k=1}^{N} \theta_k$, is replaced by $\Theta = 2\pi \cdot \mathrm{Des}(N)$, we end up with the definition (5).

In Voglis and Efthymiopoulos (1998), (6) has been generalized so that it can be used even in the case of chaotic motion. In this case, ν_θ represents an angular moment that can be expressed by the integral

$$\nu_\theta = \frac{1}{2\pi} \cdot \oint \theta \cdot S(\theta)\, \mathrm{d}\theta. \tag{8}$$

Here $S(\theta)$ is the distribution density of the values of angle θ, defined as

$$S(\theta) = \frac{\mathrm{d}N(\theta)}{N\,\mathrm{d}\theta}, \tag{9}$$

where $\mathrm{d}N(\theta)$ is the number of values of θ in the interval $(\theta, \theta + \mathrm{d}\theta)$ after N iterations. $S(\theta)$ is called the angular dynamical spectrum and for large values of N it becomes invariant along an orbit either regular or chaotic. In the case of regular motion the rotation number ν_θ converges as $1/N$ (Voglis and Efthymiopoulos 1998). In the case of chaotic motion it has been shown that the spectrum $S(\theta)$ converges to a frozen form as N increases with the law $1/\sqrt{N}$ (Voglis *et al* 1999). This property is transferred to the rotation number ν_θ.

This means that a rotation number can be defined even in the case of chaotic orbits. Thus, the definition of a rotation number in one-dimensional maps can be generalized as follows:

$$\omega = \lim_{N\to\infty} \frac{\mathrm{Des}(N)}{N}. \tag{10}$$

This definition leads to the same convergent properties of ω as ν_θ in two-dimensional maps. Indeed, we have checked that the difference of the evaluated rotation number $\omega(N)$ from the limit $\omega_* = \omega(N \to \infty)$, that is $\Delta\omega(N) = |\omega(N) - \omega_*|$, varies as $\Delta\omega \propto 1/\sqrt{N}$ for chaotic orbits outside a WOM, while as $\Delta\omega \propto 1/N$ for an orbit inside a WOM.

Namely, we consider the n intervals of N iterations each, i.e.

$$[0 - N], \qquad [N - 2N], \qquad [2N - 3N], \ldots, [(n-1)\cdot N - n\cdot N]. \tag{11}$$

We calculate the rotation number $\omega(N)$ for each one of the n intervals, in order to construct a time series for the rotation number. Then we calculate the histogram of these n values of the rotation number for two different values of N, i.e. $N_1 = 1 \times 10^4$, $N_2 = 4 \times 10^4$, at $p = 3.86$ lying on the right-hand side of the WOM of period 3 of the logistic map, as shown in figure 4(*a*). The value of n used in this figure is $n = 2 \times 10^4$.

This histogram approaches a Gaussian form with a dispersion $\delta\omega$ varying as $\delta\omega \propto 1/\sqrt{N}$ for chaotic orbits outside a WOM. This dispersion measures the thickness of the set of points $[p, \omega(p, N)]$ shown in figure 4(*b*).

In figure 4(*c*) the evolution of the current values of $\Delta\omega$ with N is demonstrated for a chaotic orbit outside the WOM of period 3 and an orbit inside this WOM. The dotted lines give the corresponding slopes -0.5 and -1 of the laws $\Delta\omega \propto 1/\sqrt{N}$ and $\Delta\omega \propto 1/N$ respectively. In figure 4(*d*) the corresponding evolution of the dispersions $\delta\omega$ with N is given, which follow the same laws respectively.

There is a simple way of finding computationally the period N_0 and the rotation number ω_0 of a WOM: Suppose that for a given value of the control parameter p the orbit belongs to a WOM of which the period N_0 we wish to find out. If the initial value of the orbit is $x = x_0$ on the highest one of the N_0 branches of the N_0th multiplicity attractor (the branch with the largest value of x) of the WOM, the values of $\omega(N)$, as the iterations N increase, behave as follows:

- In an ascent:

$$\mathrm{Des}(N+1) = \mathrm{Des}(N) \Rightarrow \frac{\mathrm{Des}(N)}{N} > \frac{\mathrm{Des}(N+1)}{N+1} \Rightarrow \omega(N) > \omega(N+1), \tag{12}$$

  i.e. $\omega(N)$ decreases to $\omega(N+1)$.
- In a descent:

$$\mathrm{Des}(N+1) = \mathrm{Des}(N) + 1 \Rightarrow \frac{\mathrm{Des}(N)}{N} < \frac{\mathrm{Des}(N+1)}{N+1} \Rightarrow \omega(N) < \omega(N+1), \tag{13}$$

  i.e. $\omega(N)$ increases to $\omega(N+1)$.

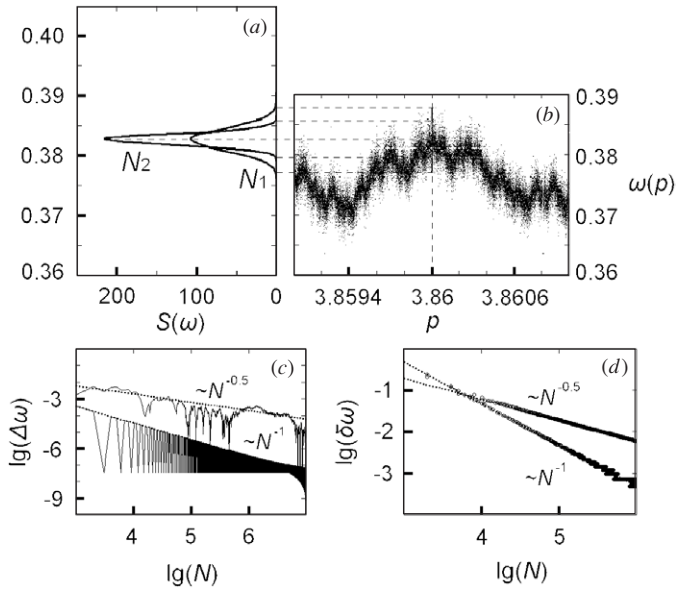

Figure 4. The histogram of $n = 2 \times 10^4$ values of the rotation number for two different values of N, i.e. $N_1 = 1 \times 10^4$, $N_2 = 4 \times 10^4$, at $p = 3.86$, is shown in (a). The respective dispersions measure the thickness of the set of points $[p, \omega(p, N)]$ shown in (b). Hereon, we set the thickness to be of about three times the dispersion of the histogram. In (c) the evolution of $\Delta\omega$ with N is demonstrated for a chaotic orbit outside the WOM of period 3 and an orbit inside this WOM. The dotted lines give the corresponding slopes -0.5 and -1 of the laws $\Delta\omega \propto 1/\sqrt{N}$ and $\Delta\omega \propto 1/N$ respectively. In (d) the corresponding evolution of the dispersions $\delta\omega$ with N, is given. (c) and (d) are depicted in a logarithmic scale.

In addition, we can easily check (e.g. in terms of the phase diagram) that although successive ascents are common, there are no successive descents at all.

Thus, we conclude that, if N_{lm} is the value of N just before any descent, then the value of $\omega(N_{lm})$ is a local minimum.

When we detect along the run of the orbit two local minima with $N_{lm,1} = N_0$ and $N_{lm,2} = 2 \cdot N_{lm,1} = 2 \cdot N_0$ then N_0 is the period of the WOM, and the precise value of the rotation number is $\omega_0 = \omega(N_0) = \omega(2 \cdot N_0)$.

Of course, this method is based on the assumption that the initial value of $x = x_0$ is sufficiently closed to the highest branch of the WOM. This specific initial value can be obtained if we start from an arbitrary initial value of x and select the maximum value of x after a sufficient number N_* of transient initial iterations.

We remark the fact that the rotation number for periodic orbits given by (5) coincides with the definition of over-rotation number given by Bloch and Misiurewicz (1997). Indeed, according to their definition, if N_{sign} is the number of times the quantity $x_{n+1} - x_n$ changes sign, where the initial value of the orbit is considered to be on a periodic attractor (either asymptotically stable or chaotic), then the over-rotation number is given by $N_{\text{sign}}/2$ divided by the period of the orbit N. The number N_{sign} is equal to the total number of local maxima and minima of the orbit occur in one period. Since the number of minima and maxima is the same, we conclude that $N_{\text{sign}}/2$ gives the number of minima, or consequently, the number of descents (we have already showed that every local minimum corresponds to a descent and vice versa).

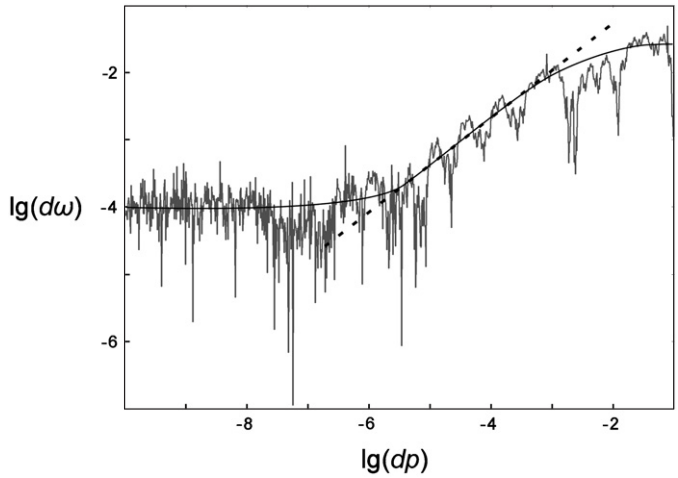

Figure 5. The dependence of $d\omega(p, N, dp)$ on dp near $p = 3.86$ (on the right-hand side of the WOM of period 3) and for $N = 10^8$, demonstrated in a logarithmic scale. The noise term is of about $\approx 10^{-4}$ and prevails for $dp < 10^{-6}$. In the region $10^{-6} < dp < 10^{-3}$, the slope which gives the fractal dimensionality is $b = 0.594 \pm 0.008$. For $dp > 10^{-3}$ large fluctuations appear, because the value of $p \pm dp$ is sufficiently different from $p = 3.86$ and various WOMs of the local area are taken into account in the calculation of $d\omega(p, N, dp)$.

Furthermore, by defining the rotation number in a way parallel to the definition given in the work of Voglis and Efthymiopoulos (1998), we were able to extend the definition in a unified way for the whole area of the chaotic zone of the bifurcation diagram, either to orbits inside a WOM (periodic or chaotic) or to (chaotic) orbits outside the WOMs.

2.3. The dependence of the rotation number on the control parameter p

As we have seen the rotation number varies in different ways with the number of iterations N inside a WOM than outside. This property makes it a useful tool in distinguishing numerically whether for a given value of p an orbit is inside or outside a WOM.

2.3.1. Inside a WOM. The value of $\omega(N)$, evaluated for N iterations inside a WOM, tends to a fixed rational number, ω_*, that characterizes the WOM for all the values of the control parameter p. In this case, we have $\omega(N) = \omega_* + \delta/N$, where δ is a constant independent of p, depending only on the initial condition. Therefore, within a WOM the value of $\omega(N)$ is independent of p.

2.3.2. Outside a WOM. For a chaotic orbit outside a WOM, the values of $\omega(N)$ depend on p. We show this as follows.

For two neighbour values of the control parameter, p and $p + dp$, we define the difference $d\omega(p, N, dp) = |\omega(p, N) - \omega(p + dp, N)|$.

In figure 5, we give an example of the dependence of $d\omega(p, N, dp)$ on dp near $p = 3.86$ (on the right-hand side of the WOM of period 3 of the logistic map) and for $N = 10^8$. In this figure, the dependence of $d\omega$ on dp, flattens for dp smaller than about $dp \approx 10^{-6}$. This is due to a threshold of noise proportional to $1/\sqrt{N}$. Since $N = 10^8$, this noise is of about $\approx 10^{-4}$. For larger values of dp however (in the region $10^{-6} < dp < 10^{-3}$), $d\omega$ is related

to the fractal dimensionality of the curve $\omega(p)$ near the particular value of $p = 3.86$. The value of the logarithmic slope $b = d\lg(\mathrm{d}\omega)/d\lg(\mathrm{d}p)$found in the particular example to be $b = 0.594 \pm 0.008$.

In general, one could write the average dependence of $\mathrm{d}\omega(p, N, \mathrm{d}p)$ on $\mathrm{d}p$ as

$$\mathrm{d}\omega(p, N, \mathrm{d}p) = a(p) \cdot \mathrm{d}p^{b(p)} + c(p)/\sqrt{N}. \tag{14}$$

Thus, for $N \to \infty$ and $\mathrm{d}p \to 0$ we have locally a fractal dimension of the curve $\omega(p)$ given by $b(p)$:

$$\lim_{\substack{N\to\infty \\ dp\to 0}} \left\{ \frac{\lg[\mathrm{d}\omega(p, N, \mathrm{d}p)]}{\lg(\mathrm{d}p)} \right\} = b(p). \tag{15}$$

Since $b(p) < 1$ (the fractal dimension is less than the dimension of the embedding space), the slope $\mathrm{d}\omega(p, N, \mathrm{d}p)/\mathrm{d}p$ cannot be defined, as $\mathrm{d}p \to 0$. Thus, the function $\omega(p, N)$ is not differentiable outside the WOMs. However, it is continuous for $N \to \infty$, while $\mathrm{d}\omega(p, N, \mathrm{d}p) \to 0$, as $\mathrm{d}p \to 0$.

Within a WOM, the parameters $a(p)$, $c(p)$ are zero and $\mathrm{d}\omega(p, N, \mathrm{d}p) = 0$.

2.3.3. Two criteria for the WOMs search. Based on the above properties of the rotation number, we present two alternative methods of investigating whether an orbit belongs to a WOM or not.

In the first method we calculate the values of the rotation number in the vicinity of the given value of p. Thus, we can check, whether there is a plateau or not, around this particular value of p.

The mathematical formulation of the corresponding criterion can be stated as follows.

If $\exists\, \Delta p > 0$, arbitrary small:

$$\forall\, \varepsilon > 0, \qquad \exists\, N_* \in \aleph : \|\omega(p + \Delta p) - \omega(p)\| < \varepsilon, \qquad \forall\, N \geqslant N_*, \tag{16}$$

then the orbit belongs to a WOM for the particular value of the control parameter p. N is the number of iterations for which the rotation number is calculated, while N_* is a minimum number of iterations needed to make the specific WOM visible. Metaphorically, this can be considered as the strength of our 'magnifying glass'.

Since $\mathrm{d}\omega(p, N, \mathrm{d}p) = 0$ everywhere within a WOM, then ε is independent of Δp. Moreover, N_* has to be sufficiently large so that it exceeds any transient initial phase, but also larger than the period N_0 of the WOM under detection. Obviously, the maximum value of Δp for which the criterion (16) holds, gives the width of the specific WOM, $\left|w_{N_0,2} - w_{N_0,1}\right|$.

For orbits outside a WOM, the negative statement of criterion (16) can be postulated.

If $\forall \Delta p > 0$:

$$\exists\, \varepsilon(\Delta p) > 0, \qquad \exists\, N_* \in \aleph : \|\omega(p + \Delta p) - \omega(p)\| \geqslant \varepsilon, \qquad \forall N \geqslant N_*, \tag{17}$$

then the orbit does not belong to a WOM for the particular value of the control parameter p.

This method requires to run an orbit for at least two neighbouring values of p.

Alternatively, a second method based on a single run of the orbit of the given p, can be used. Namely, constructing the time series of the rotation number for each one of the n intervals of (11), we examine in which way the dispersion $\delta\omega$ converges (see subsection 2.2).

2.3.4. The diagram of the rotation number depicted as a function of the control parameter p. From the above analysis we conclude that the values of $\omega(N)$ plotted as a function of p, form a plateau inside a WOM and a non-differentiable curve outside WOMs.

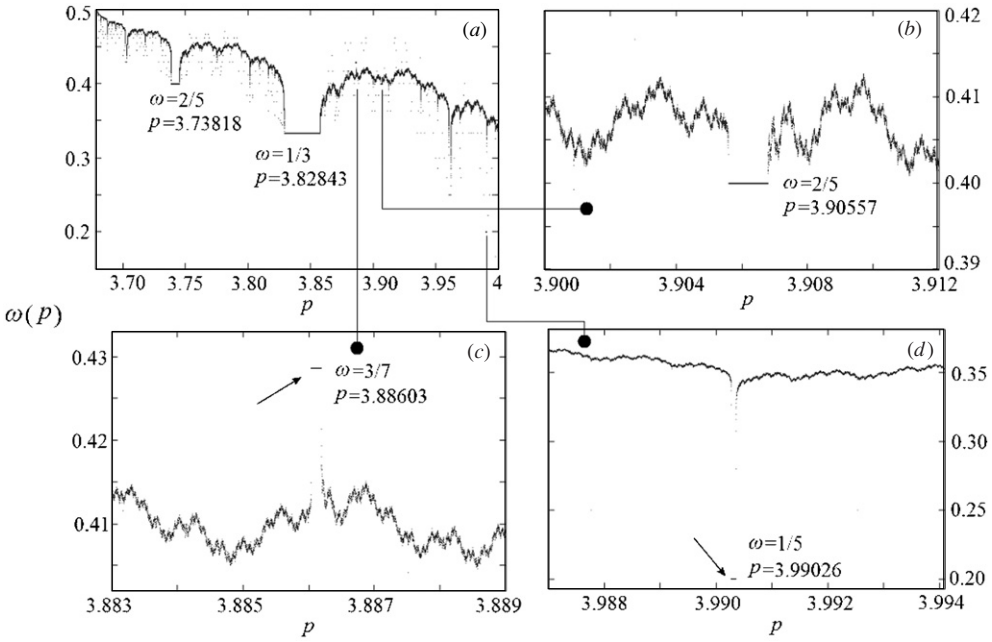

Figure 6. (*a*) The diagram of $\omega(p)$ in the case of SCB for the logistic map. The plateaux of the two WOMs with rotation numbers $\omega_1 = 1/3$ and $\omega_2 = 2/5$, described in figures 2 and 3(*a*) respectively, are indicated. The magnifying plateaux of the two WOMs with rotation numbers $\omega_3 = 2/5$ and $\omega_4 = 1/5$, described in figures 3(*b*) and (*c*) respectively, are shown in (*b*) and (*d*) respectively. A plateau lying above the non-differentiable curve, corresponding to a WOM with rotation number $\omega_5 = 3/7$, is shown in (*c*). All the values of ω are evaluated for $N = 10^6$ with step $\delta p = 10^{-6}$.

In figures 6(*a*)–(*d*) the values of ω evaluated for $N = 10^6$ are plotted as a function of p in the range of SCB of the logistic map, with step $\delta p = 10^{-6}$. In this figure, two plateaux can be clearly seen. These plateaux correspond to the rotation numbers $\omega_1 = 1/3$ and $\omega_2 = 2/5$ of the two WOMs discussed in subsection 2.1, in figures 2 and 3(*a*) respectively. The extension of each of the two plateaux covers the whole range of p of the respective WOM. The other two WOMs with the rotation numbers $\omega_3 = 2/5$ and $\omega_4 = 1/5$, described in figures 3(*b*) and (*c*) respectively, are shown as plateaux in figures 6(*b*) and (*d*) respectively (under magnification).

The thick curve between the plateaux, shown in figure 6(*a*), is a numerical approximation of the non-differentiable curve $\omega(p, N)$ formed by the chaotic orbits outside the WOMs. The thickness of this line is of the order of $1/\sqrt{N}$, as is shown in figures 4(*a*)–(*b*). In contrast, the thickness of line along the plateau is zero (a pixel), independently of N.

The non-differentiable curve is interrupted by an infinite number of plateaux that can lie on either side of this curve, corresponding to all rotation numbers of ω in the range $0 < \omega < 1/2$. As an example, in figure 6(*c*) a WOM with $\omega_5 = 3/7$ is easily discernible (under magnification) as a plateau lying above the non-differentiable curve.

Inside the SCB, the non-differentiable curve starts from $\omega(p = Q_1) = 1/2$ and terminates at $\omega(p = Q_0) = 1/3$. The value $\omega(p = Q_1) = 1/2$ is the same for any unimodal map: at $p = Q_1$, where the band merging of CB(0) and CB(1) appears, the number of descents is equal to that of the ascents, thus the rotation number is $1/2$. On the other hand, the value $\omega(p = Q_0) = 1/3$ is particularly valid for the case of the logistic map.

The non-differentiable curve is connected from both sides of plateaux, via an abrupt turn, forming a kind of a 'well'. In the case of plateaux which lie above the non-differentiable curve, the 'wells' are inverted.

The formation of these 'wells' is a consequence of intermittency and crisis, which take place for values of p slightly before and after each WOM, respectively. As the value of the control parameter p is getting closer to the boundary values $p = w_{N_0,1}$ or $p = w_{N_0,2}$ of a WOM of a period N_0, the route of a chaotic orbit is getting more similar to the respective route of a periodic orbit inside the WOM. Thus, it is characterized by a rotation number, which is getting closer to the respective rotation number of the WOM. The non-differentiable curve is getting nearer to the respective plateau of the WOM, and a well is formed.

Chaotic orbits outside any WOM are responsible for the non-differentiable behaviour of the curve of $\omega(p)$. However, 'invisible' WOMs of large period exist at any rational value of the rotation number.

It is well known that for each natural number m, there is at least one value of p where a WOM with period m exists (Arrowsmith and Place 1992, Guckenheimer *et al* 1977). Thus, the period of an infinite number of WOMs can be larger from any number of iterations we choose, and accordingly these WOMs should be 'invisible', appearing as sparse points of certain chaotic orbits.

Finally, we stress the fact that the respective diagram of $\omega(p)$ for other CBs is similar to the SCB but realized on a different scale. Note that the period of the kth generation CBs is 2^k, so that the calculation of the rotation number must be considered for each (2^k)th iteration, i.e. the time unit should be taken as 2^k iterations.

3. Further applications of the rotation number

3.1. Numerical calculation of the boundaries of a WOM, the bifurcation points and the band mergings

The calculation of the boundary points of a WOM is carried out as follows: starting from an initial value of the parameter $p_{\text{init},0}$, lying on the left-hand side of the WOM under investigation, we start increasing the parameter by a sufficiently small step δp_0. When the rotation number at a particular step first becomes equal to the rotation number of the investigated WOM, then the value of the control parameter at the previous step, $p = \tilde{p}$, approaches the left boundary of the referred WOM.

Similarly, we derive the right boundary by choosing an initial value of the parameter p_0, lying on the right-hand side of the WOM, and decreasing the parameter by the steps δp_0.

The value of p at the boundary at a desirable accuracy can be achieved by repeating the method with a smaller step $\delta p_1 < \delta p_0$ and starting from the initial value of the parameter $p_{\text{init},1} = \tilde{p}$.

By this procedure we can scan the whole of a CB. Of course, one has to keep in mind that there are more than one different WOMs characterized by the same value of rotation number.

We can use the same procedure for the calculation of the location of the bifurcation points. Consider the initial value $p_{\text{init},0}$ of the control parameter to be within the kth generation of branches in the zone of order, i.e. $p_{\text{init},0} \in (p_k, p_{k+1})$. The period of the branches is 2^k, thus the rotation number is calculated after each (2^k)th iteration. Increasing the parameter, the desirable value of p_{k+1} is the corresponding value of the parameter as soon as the rotation number becomes equal to $1/2$. Similarly, for the calculation of the location of the band mergings, we consider a value of the parameter within the p-interval of the kth generation of CBs within the chaotic zone, i.e. $p_{\text{init},0} \in (Q_{k+1}, Q_k)$. The rotation number is calculated

after each (2^k)th iteration, and as the parameter decreases, the desirable value of Q_{k+1} is the corresponding value of the parameter, as soon as the rotation number becomes equal to $1/2$. A great advantage of these procedures is that only a few iterations are usually needed in order to obtain sufficient calculations.

3.2. Numerical calculation of the percentage of the WOMs inside a CB

A direct application of the rotation number is the numerical approximation of the percentage of the WOMs in a CB, i.e. the percentage of the cumulative width of the WOMs inside a CB.

Filtering out the WOMs is based on the property of the rotation number to be constant inside each WOM, forming plateaux.

By sampling a large total number of M_{tot} points in the whole p-interval of a CB, we count the number of M_{WOM} points belonging to WOMs. Thus, the percentage of the WOMs in a CB (symbolized by WP) is

$$\text{WP} = \frac{M_{\text{WOM}}}{M_{\text{tot}}}. \tag{18}$$

The percentage, WP, in the case of SCB for the logistic map, is found to be $\text{WP} = 0.1302 \pm 0.0003$. The total number of sampling points was $M_{\text{tot}} = 2 \times 10^5$. The error was estimated by comparing the value of the WP, calculated with two different samplings $M_{\text{tot}} = 1 \times 10^5$ and $M_{\text{tot}} = 2 \times 10^5$. The number of the iterations needed for the rotation number in order to converge was $N = 1 \times 10^6$.

4. Conclusions

We have introduced a physical quantity in one-dimensional maps called rotation number, which is applicable in a unified way, either to orbits inside a WOM (periodic or chaotic) or to (chaotic) orbits outside the WOMs.

The rotation number for an orbit inside a WOM has the following three features:

- It converges with a dispersion $\delta\omega$, varying as $\delta\omega \propto 1/N$.
- It can be obtained by a simple computational way by examining the local minima of $\omega(N)$ just before any descent.
- The value of $\omega(N)$, evaluated for N iterations inside a WOM, characterizes the WOM for all the values of the control parameter p. Thus, independently of N, the values of $\omega(N)$, plotted as a function of p, form a plateau.

Respectively, the rotation number for a chaotic orbit outside a WOM is characterized by the following two features:

- It converges with a dispersion $\delta\omega$, varying as $\delta\omega \propto 1/\sqrt{N}$.
- Independently of N, the values of $\omega(N)$, plotted as a function of p outside the plateaux, form a continuous, non-differentiable curve. It has a fractal structure with a fractal dimension given locally by $b(p) < 1$ (15).

Some significant applications of the rotation number have been discussed. These include (i) two criteria of whether an orbit is contained within a WOM or not; (ii) a method of numerical calculation of the boundaries of a WOM, the locations of the bifurcation points and the band mergings; (iii) a numerical calculation of the percentage of the orbits in a CB, which belong to WOMs. In the case of SCB for the logistic map, this percentage is found to be $\text{WP} = 0.1302 \pm 0.0003$.

References

Adamopoulos A, Likothanassis S and Georgopoulos E 1997 Extracting structural characteristics of a nonlinear timeseries using genetic algorithms *Intelligent Information Systems-97 (IEEE Computer Society)* p 179

Alligood K T, Sauer T D and Yorke J A 1996 *Chaos, An Introduction to Dynamical Systems* (New York: Springer)

Arrowsmith D K and Place C M 1992 *Dynamical Systems, Differential Equations, Maps and Chaotic Behaviour* (London/Boca Raton, FL: Chapman and Hall/CRC Press)

Bloch A and Misiurewicz M 1997 New order for periodic orbits of interval maps *Ergod. Th. Dyn. Syst.* **17** 565–74

Geisel T and Nierwetberg J 1981 Universal fine structure of the chaotic region in period-doubling systems *Phys. Rev. Lett.* **47** 975–78

Guckenheimer J 1979 One dimensional dynamics *Ann. NY Acad. Sci.* **316** 76–85

Guckenheimer J and Holmes P J 1983 *Nonlinear Oscillations, Dynamical Systems, and Bifurcations of Vector Fields* (New York: Springer)

Guckenheimer J, Oster G and Ipaktchi A 1977 The dynamics of density dependent population models *J. Math. Biol.* **4** 101–47

Kapitaniak T 2000 *Chaos for Engineers* (Berlin: Springer)

Li T Y and Yorke J A 1975 Period three implies chaos *Am. Math. Mon.* **82** 985–92

Lichtenberg A J and Lieberman M A 1992 *Regular and chaotic dynamics* (New York: Springer)

Metropolis M, Stein M L and Stein P R 1973 On finite limit sets for transformations of the unit interval *J. Comb. Theory* A **15** 25–44

Peitgen H-O, Jürgens H and Saupe D 1992 *Chaos and Fractals, New Frontiers of Science* (New York: Springer)

Post T, Capel H W and Van Der Weele J P 1989 Phase-length distributions in intermittent band switching *Physica* A **160** 321–50

Schuster H G 1989 *Deterministic Chaos, An Introduction* (New York: VCH)

Voglis N, Contopoulos G and Efthymiopoulos C 1999 Detection of ordered and chaotic motion using the dynamical spectra *Celest. Mech. Dyn. Astron.* **73** 211–20

Voglis N and Efthymiopoulos C 1998 Angular dynamical spectra: a new method for determining frequencies, weak chaos and cantori *J. Phys. A: Math. Gen.* **31** 2913–28